FINITE ELEMENT SIMULATIONS OF THE MAGNETOMYOGRAM OF RAT SKELETAL MUSCLE

W.L.C. Rutten, A. Wildeman and T.H. Rozijn

Biomedical Engineering Division, Department of Electrical Engineering,

Twente University, PO Box 217, 7500 AE Enschede, The Netherlands

INTRODUCTION

A method that determines axial currents in muscle fibers non–invasively could serve to determine some important parameters of source and volume conductor rather direct (compared to EMG) and without damage to the tissue. Currents can be measured non–invasively using a magnetic method, by toroidal coils around the muscle: magnetomyogramphy (MMG). The directness of this method and the parameters to be obtained are best illustrated in a core conductor model. The axial current i_z equals

$$i_z = \frac{\sigma_i A}{v} \frac{\partial v_i}{\partial t}$$

i.e. the first derivative of the intracellular potential v_i, while action potentials are proportional to the second derivative. In this equation A is the fiber's cross section, σ_i the intracellular conductivity and v is the conduction velocity.

In an intact muscle the active fiber is embedded in a passive volume conductor which will attenuate the axial source corrent to be measured because of return axial currents in the muscle tissue, inside the toroid. Moreover, motor units have typically 75 active fibers, which travel asynchronously (different endplate positions). Also, the motor unit area in rat muscles takes about half the cross section of the muscle. This implies different depths for the 75 fibers and consequently different conductor surroundings for each fibers.

It is the purpose of this paper to present data and simulations on the dependence of magnetomyographic responses on force level, position along the muscle, depth of the source beneath the surface and the finiteness (tapering) of the muscle. This latter aspect is of utmost relevance, as action potentials are typically 10 mm wide in musles which are typically 30 mm long. See also [1].

METHODS

Magnetomyograms of rat EDL and Tibial muscle in the right hindleg were measured, using toroidal coils around the muscle. The muscle was exposed over half its length, so that the coil could be moved between origo tendon and belly of the muscle. Hindleg, muscle and coil were immersed in a bath with Ringer solution (conductivity 1.65 $\Omega^{-1}m^{-1}$). By electrical stimulation of the peroneal nerve recruitment of motor units was varied between threshold (one or two units) and maximum twitch force. The minimal input equivalent current noise of the coils was about 10^{-9} $A/\sqrt{Hz}$. They had a current noise limit of 10^{-7}–10^{-8}A in a 10 kHz bandwidth, after 100 times averaging. For other experimental details see [1]. The modeling was performed with a finite element model, basically using Ampere's law, with the active fiber(s) as input current source(s) to the model and with wedge shaped element shapes (see [1], insert of figure 3). For practical reasons the cross section of the muscle, toroid and bath were modeled as hexagonally bounded (which is as well as circularly). Conductivities could be chosen anisotropic and arbitrarily in each element. Calculations with up to 150.000 element models were performed on a HP 9000/835 computer system.

RESULTS

Figure 1 shows the peak–to–peak current of biphasic magnetic waveshapes (action fields) versus isometric twitch force of the stimulated motor units. The coil was positioned about halfway tendon and belly. Note the almost linear relationship between current and force. Figure 2 shows current as a function of coil position along the muscle, at constant force level.

Model results in figures 3 to 5 describe several aspects seen in figures 1 and 2 both qualitatively and quantitatively.

Inputs to the model are the well known analytical approximations (Rosenfalck, see [1]) for the intracellular action potential and its derivatives.

Figures 3 presents the peak–to–peak current of biphasic toroid currents due to one active muscle fiber as a function of depth of the fiber beneath the surface of the muscle, down to the center of the muscle. The coil is about halfway tendon and belly. Also peak currents of positive and negative phase are presented separately. In this case the muscle is modelled to be as long (32 mm) as in reality but yet not tapered. Figure 4 shows the results for a tapered version, both with and without the influence of tendon tissue. Figure 5 simulates the activity of one motor unit with 75 active fibers in a non–tapered muscle. Fibers are spread uniformly through half of the muscle's cross section, endplate positions are modeled realistically.

CH2936-3/90/0000-2219 $01.00

CONCLUSIONS

Finite element modelling appeared to be a very flexible way of calculating potentials and currents in a realistically shaped rat skeletal muscle. The calculations for the action field strength show that the position of the a single active fiber beneath the surface of the muscle is an important parameter. The corresponding current declines rapidly with radial position (figure 3). The toroid measures a net percentage of about 50% of the source current strength in case of superficial fibers, and of about 10% for the deepest fibers (figure 3). For a motor unit with 75 fibers, with realistically desynchronized timing–onsets, this net percentage is also 50% (Fig 5). Although a precise comparison with experiment is not possible for the absolute peak–to–peak currents (we do not know how many fibers are active in how many motor units) the calculated values are in the right order of magnitude (compare figure 5 with the most sensitive data in figure 1). Tapering of the muscle and introduction of tendon tissue yields a fall–off of current towards the tendon which was also observed qualitatively in the experiments (figure 4 and figure 2).

REFERENCES

[1] W.L.C. Rutten, A. Wildeman, B.K. van Veen and W. Wallinga, In vivo magnetomyograms of skeletal muscle. Proceedings IEEE/EMBS 11th annual international conference Seattle, 1989, pp. 981–982.

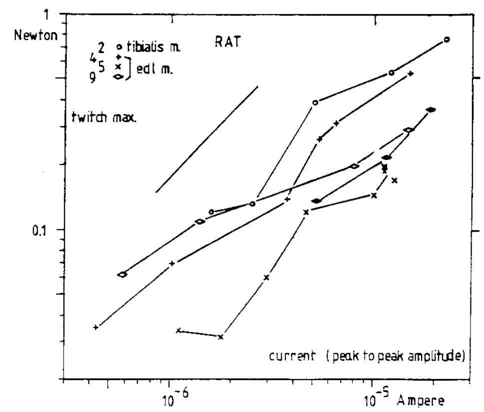

Figure 1. Peak–to–peak currents of biphasic magnetomyograms ('action fields' expressed in current) versus corresponding twitch response amplitudes for rat EDL and tibial muscles.

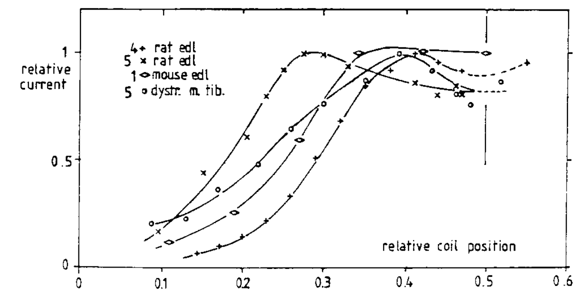

Figure 2. Relative peak–to–peak currents of magnetomyograms at a fixed force level versus relative position of the toroid coil along the muscle (left: origo tendon, right: belly of the muscle) in normal rat edl and in normal and dystrophic mouse edl and tibial muscle.

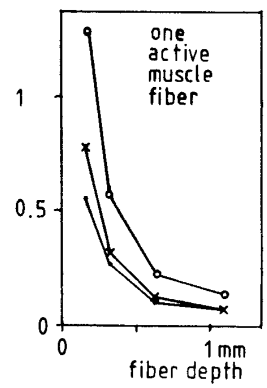

Figure 3. Calculated fall–off of peak–to–peak, positive peak and negative peak current versus depth of one active fiber beneath the surface of the muscle. The finite element model has realistic edl muscle dimensions, but is not tapered near the tendons. The toroid is positioned halfway tendon and belly.

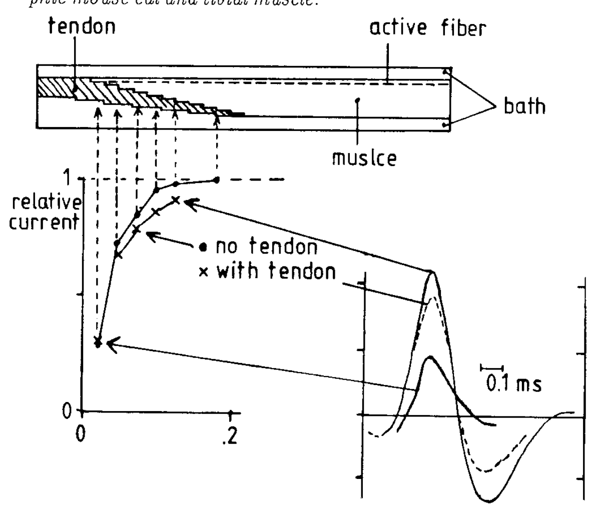

Figure 4. The fall–off of current along the muscle as a result of tapering and tendon tissue.

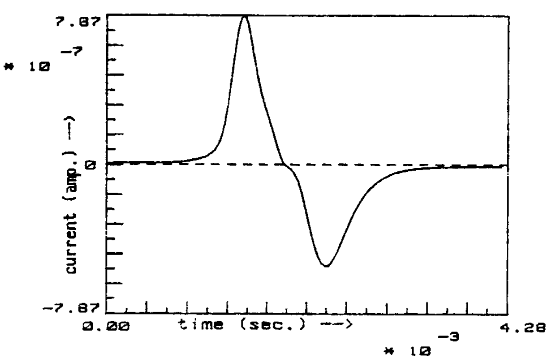

Figure 5. MMG waveforms as measured by the toroid (halfway tendon and belly) due to activity of one motor unit with 75 fibers. The endplate region has been modeled realistically for desynchronized start of waveforms. The muscle has realistic edl dimensions, but is not tapered.